ISSN(Online) : 2319-8753
ISSN (Print) : 2347-6710

International Journal of Innovative Research in Science, Engineering and Technology

(An ISO 3297: 2007 Certified Organization)

Vol. 5, Issue 4, April 2016

Contraction of High Eccentricity Satellite Orbits Using Uniformly Regular KS Canonical Elements in an Oblate Diurnally Varying Atmosphere

P.S.Rajendran[1], M. Xavier James Raj[2]

Research Scholar, Manonmaniam Sundaranar University, Tirunelveli, Tamil Nadu, India and

Associate Professor, College of Engineering, Thiruvanathapuram, Kerala, India[1]

Head, OAS, Applied Mathematics Division, Vikram Sarabhai Space Centre, Thiruvanathapuram, India[2]

ABSTRACT: A new non-singular analytical theory for the motion of near Earth high eccentricity satellite orbits is developed for long-term motion in terms of uniformly regular KS canonical elements using the oblate diurnally varying atmosphere with constant density scale height. The analytical solutions are generated using series expansion method with a new independent variable λ. The series expansions include up to fourth-order terms in λ and c (a small parameter dependent on the flattening of the atmosphere). Only two of the nine equations are solved analytically to compute the state vector and change in energy at the end of each revolution, due to symmetry in the equations of motion. Comparison with the numerically integrated values for the important orbital parameters semi major axis and eccentricity, which determine the size and shape of the orbit up to 100 revolutions, shows the accuracy of the analytical theory.

KEYWORDS: Non-singular analytical solution; Orbital elements; KS canonical elements; Oblate diurnal atmosphere.

1. INTRODUCTION

Accurate orbit prediction of Earth's artificial satellite is an important requirement for mission planning, space craft navigation, satellite geodesy, re-entry predictions, orbital lifetime estimations, collision avoidance, maneuver strategy, etc. The satellites on Low Earth Orbits (LEO), mainly experiencing the influence of air drag, which can have perturbing effect of many times than other perturbing forces. The effects of atmosphere are difficult to determine, since the atmospheric density under goes large fluctuations. Due to atmospheric resistance, there will be a continuous loss of kinetic energy from the satellite to the atmosphere, causing drop in satellite altitude. The selection of an appropriate atmospheric model has of great significance in the study of satellite motion.

Orbits like Geostationary Transfer Orbits (GTO) are highly elliptical with apogee altitude of about 35,700 km and low perigee altitude, which passes through high atmospheric regions. These orbits have large variations in velocity due to perturbations during a revolution. Hence, the computational efficiency of the numerical methods decreases. So, during the mission planning, the analytical solutions are preferred.

Many transformations have emerged to stabilize the non linear equations of motion, either to reduce numerical errors or allowing the use of large integration step sizes, or both. One such transformation is KS transformation [1], which regularize the equation of motion and reduced it into linear equations. KS method [2] is found to be a powerful method with respect to any type of perturbing forces [3]. Sharma and Xavier James Raj [4, 5] developed an analytical theory for high eccentricity orbits using oblate atmosphere with variation of density scale height in terms of KS elements.

The uniformly regular KS canonical equations are, a particular canonical form of the KS differential equations, where all the ten KS Canonical elements α_i and β_i are constant for unperturbed motion. These equations permit the

ISSN(Online) : 2319-8753
ISSN (Print) : 2347-6710

International Journal of Innovative Research in Science, Engineering and Technology

(An ISO 3297: 2007 Certified Organization)

Vol. 5, Issue 4, April 2016

uniform formulation of the basic laws of elliptic, parabolic and hyperbolic motion [2]. The equations were utilized to generate number of analytical theories [6, 7, 8, 9] with different atmospheric models and proved that uniformly regular KS canonical theory is better than the existing analytical theories including KS theory. But all are only for the low eccentricity orbits (e < 0.2). For high eccentricity orbits (e > 0.2) these equations are used analytically to predict orbit only with oblate atmosphere [10,11,12].

In this paper, a new non singular analytical theory is developed for the motion of high eccentricity orbits (e > 0.2) using uniformly regular KS canonical elements in the realistic atmosphere i.e., oblate diurnally varying atmosphere with constant scale height. The analytical solutions are generated with series expansion method using a new independent variable λ introduced by Sterne [13]. Due to symmetry, only two of the ten equations need to be solved analytically to get the complete analytical solutions. Comparison of the results up to 100 revolutions with numerically integrated values for the important orbital parameters semi-major axis and eccentricity for a wide range of perigee height, eccentricity and inclination shows the accuracy of the present theory.

II. RELATED WORK

The authors developed an analytical theory for orbit predictions for high eccentricity (e > 0.2) orbits with uniformly regular KS canonical elements using oblate atmosphere with constant scale height [10]. Anitha and Sharma obtained analytical solutions for uniformly regular KS canonical elements using oblate atmosphere with variation in scale height for high eccentricity orbits [11]. The authors integrated low eccentricity theory with high eccentricity theory and obtained the analytical solutions for low and high eccentricity orbits (0 < e < 1) using oblate atmosphere with scale height variation [12] in terms of uniformly regular KS canonical elements. The present paper deals with the analytical solutions for high eccentricity orbits using oblate diurnally varying atmosphere with constant scale height in terms of uniformly regular KS canonical elements.

III. EQUATIONS OF MOTION

If A_k and B_k are the canonical forces attached to the system of equations, then the canonical equations of motion (Stiefel and Scheifele, 1971, p250)

$$\frac{d\beta_k}{ds} = \frac{\partial H}{\partial \alpha_k} - B_k, \frac{\mathrm{d}\alpha_k}{\mathrm{ds}} = -\frac{\partial H}{\partial \alpha_k} + \mathrm{A}_k, \tag{1}$$

with $$A_k = \sum_{j=0}^{4} W_j \frac{\partial u_k}{\partial \beta_k}, \; B_k = \sum_{j=0}^{4} W_j \frac{\partial u_k}{\partial \alpha_k} \qquad (k = 0,1,2,3,4) \tag{2}$$

where, $$W_0 = -\frac{r}{2}(\vec{v}, D), \; W = \frac{r}{2} L^T(\vec{u})\vec{D} \quad \text{where } W = (W_1, W_2, W_3, W_4)^T \tag{3}$$

If $\vec{D}$ is the aerodynamic drag force per unit mass on a satellite of mass m (King-Hele, 1987), then

$$\vec{D} = -0.5\rho\delta|\vec{v}|\vec{v} \tag{4}$$

where ρ is the atmospheric density, $\delta = FAC_D / m$, with $F = [1 - r_{p_0} \Lambda \cos i_0 / v_{p_0}]^2$, i_0 is the initial inclination, v_{p_0} is the velocity at the initial perigee, C_D and A are, respectively, the drag coefficient and the effective area of the satellite, Λ is the rotational rate of the atmosphere about the Earth's axis, r_{p_0} is the initial perigee radius,

If we consider only the canonical forces, then the Eqs. (1) become

ISSN(Online) : 2319-8753
ISSN (Print) : 2347-6710

International Journal of Innovative Research in Science, Engineering and Technology

(An ISO 3297: 2007 Certified Organization)

Vol. 5, Issue 4, April 2016

$$\frac{d\beta_k}{ds} = -B_k,\ \frac{d\alpha_k}{ds} = A_k, \qquad (k = 0,1,2,3,4) \tag{5}$$

Substituting $L^T(u)\vec{v} = 2\vec{w}$ and the expressions of $\vec{D}$ from Eq. (4) in Eq. (3), we get

$$W_0 = 0.25\rho\,\delta\, r|\vec{v}|^3,\ W_j = -0.5\,\rho\delta\, r|\vec{v}|w_j \qquad (j = 1,2,3,4) \tag{6}$$

Substituting $r = a(1 - e\cos E)$ and the expression for w_k and partial derivative of u_k (Stiefel and Scheifele, 1971, p251)) in Eqs. (3) and substituting in the Eqs. (2) and simplifying, we get

$$A_0 = 0.25\rho\delta|\vec{v}|\mu(1 + e\cos E),$$

$$A_j = -B_j = 0.25\rho\delta|\vec{v}|[S_{0j} + S_{1j}\cos E + S_{2j}\cos 2E + S_{3j}\sin E + S_{4j}\sin 2E + S_{5j}E + S_{6j}E\cos E] \tag{7}$$

(j = 1,2,3,4).

where the coefficients S_{ij} are given in the Appendix-I

Hence, using (7) and $E = 2\sqrt{\alpha_0}\,s$ eqn. of motion (5) in terms of eccentric anomaly becomes

$$\frac{d\alpha_0}{dE} = \frac{1}{8\sqrt{\alpha_0}}\rho\delta|\vec{v}|\mu[1 + e\cos E]$$

$$\frac{d\alpha_j}{dE} = \frac{1}{8\sqrt{\alpha_0}}\rho\delta|\vec{v}|[S_{0j} + S_{1j}\cos E + S_{2j}\cos 2E + S_{3j}\sin E + S_{4j}\sin 2E + S_{5j}E + S_{6j}E\cos E] \tag{8}$$

with $\alpha_{j+4} = \beta_j$ for j = 1, 2, 3, 4 .

IV. OBLATE DIURNALLY VARYING ATMOSPHERE

The air density at a given height depends upon the geographic latitude, longitude and the Sun's location. So, in reality the atmospheric density undergoes a variation between day and night. The day to night variation in density is linked with the day to night temperature variation, may be referred as 'day time bulge' of density. The daytime bulge is caused by the constant heating of the atmosphere on the sunlit side of the Earth. Hence, the density depends primarily on the angular distance from the center of the bulge.

If the air density at a given height is assumed to be depending on the angular distance from the center of the bulge, a sinusoidal variation ρ, then ρ may be written as [14]

$$\rho = k\left[1 + FA\left(\frac{\cos E - e}{1 - \cos E}\right) + FB\left(\frac{\sqrt{1-e^2}\sin E}{1 - \cos E}\right)\right]\exp(z\cos E)\exp\{c\cos 2(\omega + \theta) + O(c\varepsilon)\}, \tag{9}$$

with

$$k = \rho_{p_0}\exp(\bar{\beta}\, r_{p_0} - c\cos 2\omega_0), \qquad c = \frac{1}{2}\varepsilon\beta\, r_{p_0}\sin^2 i, \qquad z = \beta\, a\, e.$$

$$F = (f - 1)/(f + 1) \qquad f = \rho_{\max}/\rho_{\min} \qquad \beta = H_0^{-1}$$

ISSN(Online) : 2319-8753
ISSN (Print) : 2347-6710

International Journal of Innovative Research in Science, Engineering and Technology

(An ISO 3297: 2007 Certified Organization)

Vol. 5, Issue 4, April 2016

$A = \sin\delta_B \sin i \sin\omega + \cos\delta_B \{\cos(\Omega - \alpha_B)\cos\omega - \cos i \sin(\Omega - \alpha_B)\sin\omega\}$,
$B = \sin\delta_B \sin i \cos\omega - \cos\delta_B \{\cos(\Omega - \alpha_B)\sin\omega + \cos i \sin(\Omega - \alpha_B)\cos\omega\}$,
$\alpha_B = \alpha_s + \lambda$, $\delta_B = \delta_s$ where, (α_s, δ_s) and (α_B, δ_B) are the right ascension and declination of the Sun and the center of the day time bulge.

V. ANALYTICAL INTEGRATION

For high eccentricity orbits, introduce a new independent variable λ defined in [13] as $\cos E = 1 - \lambda^2/z$, where $z = ae/H$

Substituting this and expanding up to 8th power in $K = \frac{\lambda}{s}$ we get the atmosphere as {

$$\rho = k_1 \exp(-\lambda^2)(1 + F_0 + F_1 K + F_2 K^2 + F_3 K^3 + F_4 K^4 + F_5 K^5 + F_6 K^6 + F_7 K^7 + F_8 K^8) \quad (10)$$

where $k_1 = k \exp\{\beta a e\}$ and the coefficients F_i's are given in the Appendix-I.

Expanding $|\vec{v}| = \sqrt{\frac{\mu(1 + e\cos E)}{a(1 - e\cos E)}}$ appearing in equation of motion (8) up to fourth order terms in λ with the help of $\cos E = 1 - \lambda^2/z$ we get

$$|\vec{v}| = \sqrt{\frac{\mu(1+e)}{a(1-e)}}\left[1 + V_1\lambda + +V_2\lambda^2 + V_3\lambda^3 + V_4\lambda^4\right], \quad (11)$$

where, the coefficients V_i are given in the Appendix-I.

Substituting Eqs., (10) and (11) into the equations of motion (8) and expanding the resultant integrands in powers of $\frac{\lambda}{s}$, we get

$$\frac{d\alpha_0}{d\lambda} = \frac{1}{8\sqrt{\alpha_0}} k_1 \delta\mu e^{-\lambda^2} \sqrt{\frac{2\mu}{za}} \sum_{i=0}^{8} P_i \left(\frac{\lambda}{s}\right)^i, \quad \frac{d\alpha_i}{d\lambda} = \frac{1}{8\sqrt{\alpha_0}} k_1 \delta e^{-\lambda^2} \sqrt{\frac{2\mu}{za}} \sum_{i=0}^{8} M_i \left(\frac{\lambda}{s}\right)^i \quad (12)$$

with $\alpha_{i+4} = \beta_i$, for i = 1,2,3,4.

where the coefficients P_i and M_i are provided in Appendix-II .

Changes in α_i and β_i during one revolution is obtained by integrating Eqs. (12) from 0 to $\sqrt{2z}$ as

$$\Delta\alpha_0 = \frac{k_1}{8\sqrt{\alpha_0}} \delta\mu \sqrt{\frac{2\mu}{az}} \sum_{i=0}^{8} \int_0^{\sqrt{2z}} e^{-\lambda^2} P_i \left(\frac{\lambda}{s}\right)^i d\lambda, \quad \Delta\alpha_i = \frac{k_1}{8\sqrt{\alpha_0}} \delta \sqrt{\frac{2\mu}{az}} \sum_{i=0}^{8} \int_0^{\sqrt{2z}} e^{-\lambda^2} M_i \left(\frac{\lambda}{s}\right)^i d\lambda \quad (13)$$

with $\alpha_{i+4} = \beta_i$ for i = 1,2,3,4.

For $e > 0.2$, the value of $\sqrt{2z}$ exceeds 6 and the limits $\sqrt{2z}$ can be replaced with ∞ with relative error less than 10^{-16} [15]

ISSN(Online) : 2319-8753
ISSN (Print) : 2347-6710

International Journal of Innovative Research in Science, Engineering and Technology

(An ISO 3297: 2007 Certified Organization)

Vol. 5, Issue 4, April 2016

Also if we write $\int_0^\infty \lambda^{2n} \exp(-\lambda^2) d\lambda = G_n$, then $G_n = \frac{1}{2}(2n-1)G_{n-1}$ *for* $n \geq 1$.

Since $G_0 = \frac{1}{2}\sqrt{\pi}$, we have $G_1 = \frac{1}{4}\sqrt{\pi}$, $G_2 = \frac{3}{8}\sqrt{\pi}$, $G_3 = \frac{15}{16}\sqrt{\pi}$, $G_4 = \frac{105}{32}\sqrt{\pi}$,

Employing the above integrals and simplifying, (13) becomes,

$$\Delta\alpha_0 = \frac{k_1}{8\sqrt{\alpha_0}}\delta\mu\sqrt{\frac{2\mu}{az}}\left\{\frac{\sqrt{\pi}}{16}\left[8P_0 + 4\frac{P_2}{s^2} + 6\frac{P_4}{s^4} + 15\frac{P_6}{s^6} + \frac{105}{2}\frac{P_8}{s^8}\right] + \frac{1}{2}\left[\frac{P_1}{s} + \frac{P_3}{s^3} + 2\frac{P_5}{s^5} + 6\frac{P_7}{s^7}\right]\right\}$$

$$\Delta\alpha_i = \frac{k_1}{8\sqrt{\alpha_0}}\delta\mu\sqrt{\frac{2\mu}{az}}\left\{\frac{\sqrt{\pi}}{16}\left[8M_0 + 4\frac{M_2}{s^2} + 6\frac{M_4}{s^4} + 15\frac{M_6}{s^6} + \frac{105}{2}\frac{M_8}{s^8}\right] + \frac{1}{2}\left[\frac{M_1}{s} + \frac{M_3}{s^3} + 2\frac{M_5}{s^5} + 6\frac{M_7}{s^7}\right]\right\}$$

with $\alpha_{i+4} = \beta_i$ for $k = 1, 2, 3, 4$. (14)

VI. NUMERICAL RESULTS

To compute $\Delta\alpha_k$ and $\Delta\beta_k$ ($k = 0, 1, 2, 3, 4$) at the end of each revolution, we have programmed equations (14). Once $\Delta\alpha_k$ and $\Delta\beta_k$ are known, then α_k and β_k can be updated. Thus u_k and w_k can be computed, then the position and velocity vector are computed from the following relations: $(x, y, z) = L(\vec{u})\vec{u}$ and $(\dot{x}, \dot{y}, \dot{z}) = 2L(\vec{u})\vec{w}/r$, which are then converted in to the osculating orbital elements. The value of the ballistic coefficient ($b_n = AC_D/m$) is chosen as 50.0 kg/m^2. The Earth's equatorial radius R_E, ε, Λ, μ are taken as 6378.135 km, 0.00335, 1.2, 398600.8 km^{3}s^{-2}, respectively. Jacchia (1977) atmospheric density model is employed to compute the values of density and density scale height. Arbitrarily, 22 August 1995 is chosen as the initial epoch. The value of 10.7 cm solar flux (F10.7) is used as 150.0 and averaged geomagnetic index (A_p) is taken as 10. The KS Equations of motion are numerically integrated (NUM) with a small step size of half degree in the eccentric anomaly (E), with a fixed step size fourth- order Runge-Kutta-Gill method to obtain the numerical solutions. To study the effect of the drag force, detailed numerical simulations are carried out with respect to orbits with variations in eccentricity, inclination and perigee height. The values of argument of perigee (ω), right ascension of ascending node (Ω) and E are taken as 60, 30 and 0 degrees, respectively. Table-1 provides the numerically integrated (NUM) and analytically (ANAL) computed values of semi major axis (a) and eccentricity (e) after 100 revolutions with percentage error [100(NUM-ANAL)/NUM] for the orbits with initial perigee height of 200km, inclination of 35° and eccentricity varies from 0.2 to 0.9. It is observed that the percentage errors are very low for both parameters. A maximum percentage error of 0.008 is noted.

Table-1: Numerical and Analytical values of semi major axis and eccentricity after 100 revolutions for the initial perigee height of 200 km and inclination of 35° with variation in eccentricity

e	a (km)		e		% error	
	NUM	ANAL	NUM	ANAL	a	e
0.2	8200.062	8199.955	0.19781	0.19780	0.001	0.005
0.3	9370.185	9369.959	0.29797	0.29796	0.002	0.006
0.4	10927.827	10927.385	0.39804	0.39802	0.004	0.006
0.5	13093.383	13092.456	0.49804	0.49801	0.007	0.007
0.6	16365.014	16363.737	0.59804	0.59800	0.008	0.007
0.7	21778.086	21777.110	0.69795	0.69793	0.005	0.004
0.8	32551.568	32553.160	0.79794	0.79793	-0.005	0.001
0.9	64407.289	64411.854	0.89785	0.89787	-0.007	-0.003

ISSN(Online) : 2319-8753
ISSN (Print) : 2347-6710

International Journal of Innovative Research in Science, Engineering and Technology

(An ISO 3297: 2007 Certified Organization)

Vol. 5, Issue 4, April 2016

Table 2 provides the numerically integrated (NUM) and analytically (ANAL) computed values of semi major axis and eccentricity after 100 revolutions for the orbits with initial eccentricity of 0.5, inclination of 75^o and perigee height varies from 160 to 300 km. After 100 revolutions the maximum absolute percentage error noted is only 0.03 for both parameters. Table 3 provides the numerically integrated (NUM) and analytically (ANAL) computed values of semi major axis and eccentricity after 100 revolution for the orbits with initial perigee height of 200 km, eccentricity of 0.5 and inclination varies from 1 to 90 degrees. It is noted that after 100 revolutions the maximum absolute percentage error is 0.009 for both semi major axis and eccentricity.

Table-2: Numerical and Analytical values of semimajor axis and eccentricity after 100 revolutions for the initial eccentricity of 0.5 and inclination of 75^o with variation in perigee height

Hp (km)	a (km)		e		% error	
	NUM	ANAL	NUM	ANAL	a	e
160	12896.275	12900.041	0.49342	0.49356	-0.029	-0.030
180	13012.935	13014.575	0.49646	0.49648	-0.013	-0.005
200	13100.061	13100.754	0.49788	0.49786	-0.005	0.004
220	13149.937	13149.352	0.49862	0.49860	0.004	0.004
240	13201.788	13201.136	0.49907	0.49905	0.005	0.005
260	13249.308	13248.693	0.49936	0.49934	0.005	0.005
280	13294.267	13293.709	0.49955	0.49953	0.004	0.004
300	13337.620	13337.141	0.49968	0.49966	0.004	0.004

Table-3: Numerical and Analytical values of semimajor axis and eccentricity after 100 revolutions for the initial perigee height of 200 km and eccentricity of 0.5 with variation in inclination

i (deg.)	a (km)		e		% error	
	NUM	ANAL	NUM	ANAL	a	e
1	13104.541	13105.679	0.49807	0.49803	-0.009	0.009
10	13104.459	13105.562	0.49807	0.49803	-0.008	0.008
20	13104.218	13105.253	0.49806	0.49802	-0.008	0.008
30	13103.804	13104.765	0.49804	0.49800	-0.007	0.007
40	13103.208	13104.107	0.49801	0.49798	-0.007	0.007
50	13102.442	13103.296	0.49798	0.49795	-0.007	0.007
60	13101.532	13102.351	0.49794	0.49791	-0.006	0.006
70	13100.536	13101.296	0.49790	0.49788	-0.006	0.006
80	13099.523	13100.158	0.49786	0.49784	-0.005	0.005
90	13098.784	13099.157	0.49782	0.49781	-0.003	0.003

Figures 1 to 3 depict the differences between the numerically integrated and analytically computed values for the important orbital elements semi-major axis (a) and eccentricity (e), after 100 revolutions, corresponding to Tables 1 to 3. It is noticed that the differences are small.

From Tables 1 to 3 and Figures 1 to 3, it is clear that the numerically integrated values are well matched with analytically computed values for the important orbital elements semi-major axis and eccentricity, which define the size and shape of the orbit after 100 revolutions, for the wide range of perigee height, eccentricity and inclination.

ISSN(Online) : 2319-8753
ISSN (Print) : 2347-6710

International Journal of Innovative Research in Science, Engineering and Technology

(An ISO 3297: 2007 Certified Organization)

Vol. 5, Issue 4, April 2016

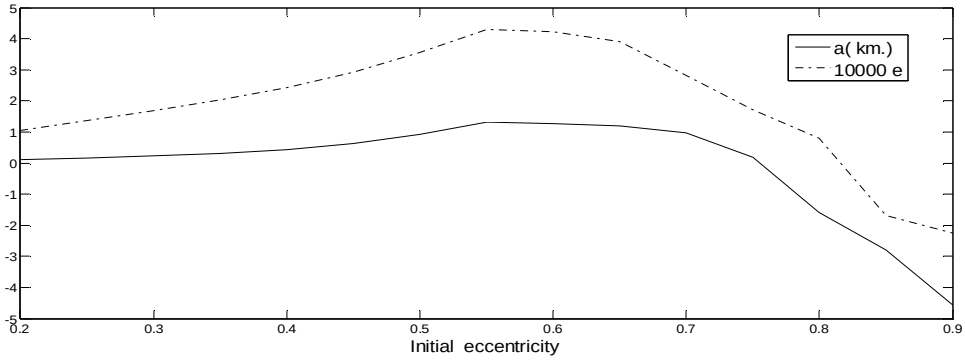

Fig.1: Variation of difference between numerically and analytical values of semi major axis and eccentricity after 100 revolutions for the orbits with initial perigee height of 200 km and inclination of 35°.

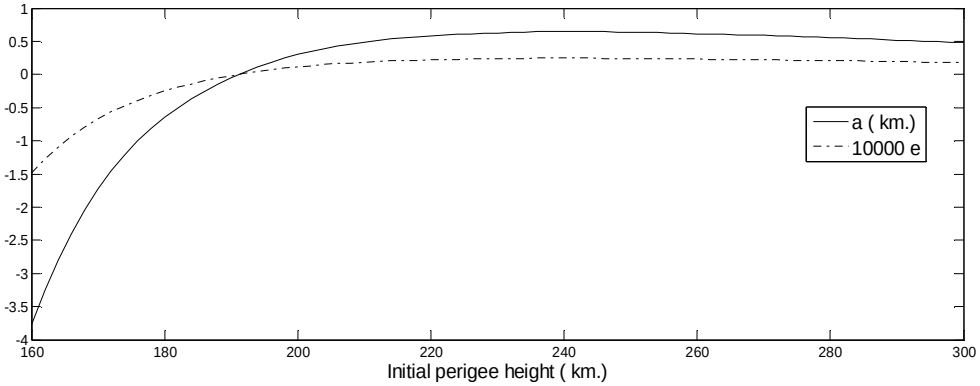

Fig.2: Variation of difference between numerically and analytical values of semi major axis and eccentricity after 100 revolutions for the orbits with initial eccentricity of 0.5 and inclination of 75°.

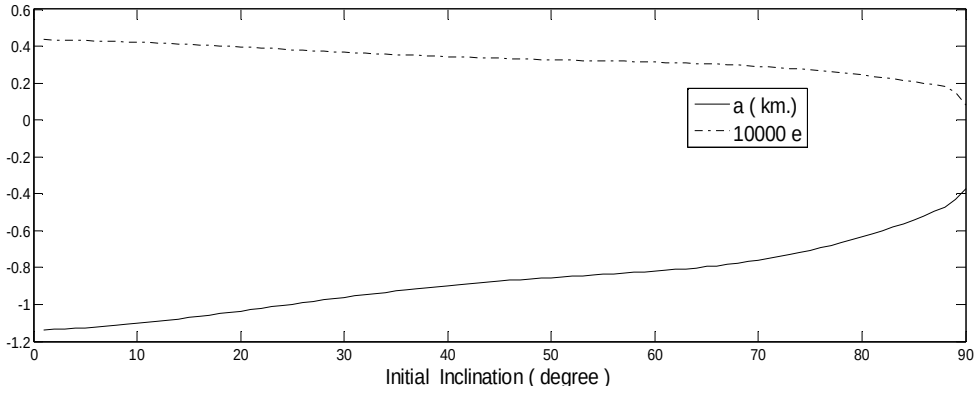

Fig.3: Variation of difference between numerically and analytical values of semi major axis and eccentricity after 100 revolutions for the orbits with initial perigee height of 200 km and eccentricity of 0.5.

ISSN(Online) : 2319-8753
ISSN (Print) : 2347-6710

International Journal of Innovative Research in Science, Engineering and Technology

(An ISO 3297: 2007 Certified Organization)

Vol. 5, Issue 4, April 2016

V. CONCLUSION

The uniformly regular KS canonical element equations are integrated analytically by a series expansion method with air drag force, by assuming an analytical oblate exponential atmosphere with diurnal variation for high eccentricity orbits. Only two of the nine equations are solved analytically to compute the state vector and change in energy at the end of each revolution, due to symmetry in the equations of motion. Comparisons of the present analytical solution, with numerically integrated values, shows that the present theory provides accurate estimates for the important orbital parameters semi-major axis and eccentricity over a wide range of perigee height, eccentricity and inclination.

REFERENCES

[1] Kustaanheimo, P and Stiefel, E. L., "Perturbation Theory of Kepler Motion Based on Spinor regularization", J Reine Angew Math., 218: 204-219, 1965.

[2] Stiefel, E.L., and Scheifele, G., Linear and Regular Celestial Mechanics, Berlin, Springer, 1971.

[3] Graf, Jr. O.F., Mueller, A., and Starke, S., "The Method of Averages Applied to the KS Differential Equations", NASA-CR-151607, 1977.

[4] Sharma, R.K., and Xavier James Raj, M., "Fourth-order theories for orbit predictions for low-and high-eccentricity orbits in an oblate atmosphere with scale height dependent on altitude", Acta Astronautica, 65, 1336-1344, 2009.

[5] Sharma, R.K., and Xavier James Raj, M., "Analytical Approach Using KS Elements to High Eccentricity Orbit Prediction Including Drag", Acta Astronautica, 66, 864-870, 2010.

[6] Xavier James Raj, M., and Sharma, R. K., "Analytical Orbit Predictions with Air Drag Using KS Uniformly Regular Canonical Elements", Planetary and Space Science, 54, 310-316, 2006.

[7] Xavier James Raj, M., and Sharma, R. K., "Contraction of Satellite Orbits Using KS Uniformly Regular Canonical Elements in an Oblate Diurnally Varying Atmosphere". Planetary and Space Science, 55, 1388-1397, 2007.

[8] Xavier James Raj, M., and Sharma, R. K., "Contraction of near-Earth Satellite Orbits Using Uniformly Regular KS Canonical Elements in an Oblate Atmosphere with Density Scale Height Variation with Altitude", Planetary and Space Science, Volume 57, Issue 1, 34- 41,2009.

[9] Xavier James Raj, M., and Sharma, R. K., "Prediction of Satellite Orbits Contraction due to Diurnally Varying Oblate Atmosphere and Altitude Dependent Scale Height using KS Canonical Elements", Planetary and Space Science, 57, 1312-1320, 2009.

[10] Rajendran, P.S. and Xavier James Raj, M., "Analytical orbit prediction for high eccentricity orbits with oblate atmosphere using uniformly regular KS canonical elements", International Journal of Math. Sci. & Engg. Appls.(IJMSEA),Vol.7, No.6, 239-259, 2103.

[11] Anitha and Sharma, R.K., "Decay of high eccentricity satellite orbits with air drag using uniformly regular KS canonical elements", Acta Astronautica, 68, 1865-1871, 2011.

[12] Rajendran, P.S. and Xavier James Raj, M., "Analytical orbit predictions for low and high eccentricity orbits using oblate atmosphere with scale height variations in terms of uniformly regular KS canonical elements", Bull. Cal. Math. Soc., 107, (1) 89-104, 2015.

[13] Sterne, T.E., "An Introduction to Celestial Mechanics", Ch.4. Interscience, New York, 1960.

[14] Swinerd,G.G. and Boulton,W.J., "Contraction of satellite orbits in an oblate atmosphere with a diurnal density variation", Proc. R. Soc. Lond. A 383, 127-145 1982

[15] King-Hele, D.G., "Satellite orbits in an atmosphere: Theory and Applications." Blackie and Son Ltd., London, 1987.

Appendix I

$S_{0j} = \mu P_{2j} + a Q_{2j} + e(\mu P_{0j} - a Q_{oj})/2$, $S_{1j} = \mu P_{0j} + a Q_{0j} + e(\mu P_{2j} - a Q_{2j})$,

$S_{2j} = e(\mu P_{0j} - a Q_{oj})/2$, $S_{3j} = \mu P_{1j} + a Q_{1j}$,

$S_{4j} = e(\mu P_{1j} - a Q_{1j})/2$, $S_{5j} = \mu P_{3j}$, $S_{6j} = e \mu P_{3j}$.

For j =1, 2, 3, 4,

For	P_{oj}	P_{1j}	P_{2j}	P_{3j}	Q_{0j}	Q_{1j}	Q_{2j}
A_j	$\alpha_j / (4\alpha_0)$	$-\beta_j / (4\alpha_0^{1.5})$	$-\alpha_j / (4\alpha_0)$	$\beta_j / (4\alpha_0^{1.5})$	α_j	$-\beta_j / (\alpha_0^{0.5})$	$-\alpha_j$
B_j	$-\beta_j / (4\alpha_0)$	$-\alpha_j / (4\alpha_0^{0.5})$	$\beta_j / (4\alpha_0)$	$\alpha_j / (4\alpha_0^{0.5})$	$-\beta_j$	$-\alpha_j (\alpha_0^{0.5})$	$-\beta_j$

$F_0 = H_0 R_0$, $F_1 = H_0 R_1 + H_1 R_0$, $F_2 = H_0 R_2 + H_1 R_1 + H_2 R_0$,

$F_3 = H_0 R_3 + H_1 R_2 + H_2 R_1 + H_3 R_0$, $F_4 = H_0 R_4 + H_1 R_3 + H_2 R_2 + H_3 R_1 + H_4 R_0$,

ISSN(Online) : 2319-8753
ISSN (Print) : 2347-6710

International Journal of Innovative Research in Science, Engineering and Technology

(An ISO 3297: 2007 Certified Organization)

Vol. 5, Issue 4, April 2016

$$F_5 = H_0R_5 + H_1R_4 + H_2R_3 + H_3R_2 + H_4R_1 + H_5R_0,$$
$$F_6 = H_0R_6 + H_1R_5 + H_2R_4 + H_3R_3 + H_4R_2 + H_5R_1 + H_6R_0,$$
$$F_7 = H_0R_7 + H_1R_6 + H_2R_5 + H_3R_4 + H_4R_3 + H_5R_2 + H_6R_1 + H_7R_0,$$
$$F_8 = H_0R_8 + H_1R_7 + H_2R_6 + H_3R_5 + H_4R_4 + H_5R_3 + H_6R_2 + H_7R_1 + H_8R_0,$$
$$R_0 = 1$$
$$R_1 = -2c\sin 2\omega, \qquad R_2 = 2c[c\sin^2 2\omega - \cos 2\omega],$$
$$R_3 = -\frac{c\sin 2\omega}{12(1+e)}\left[16c(1+e)\{c\sin^2 2\omega - 3\cos 2\omega\} - 3(5+7e)\right],$$
$$R_4 = \frac{c}{6(1+e)}\left[\begin{array}{l} 4c(1+e)\{c\sin^2 2\omega(c\sin^2 2\omega - 6\cos 2\omega) + 3\cos^2 2\omega\} \\ \quad -3c\sin^2 2\omega(7e+5) + \cos 2\omega(9e+3) \end{array}\right],$$
$$R_5 = \frac{c\sin 2\omega}{192(1+e)^2}\left[\begin{array}{l} \{512c^3\cos 2\omega(1+e)^2 + 96c^2(7e^2+12e+5)\}\sin^3 2\omega \\ \quad -96c\cos 2\omega\{(7+20e+13e^2) + 8c(1+e)^2\cos 2\omega\} \\ -3(7+74e+79e^2) \end{array}\right],$$
$$R_6 = \frac{-c}{6(1+e)^2}\left[\begin{array}{l} c\sin^2 2\omega\{2c^2\sin^2 2\omega(7e^2+12e+5) - 24c^2\cos^2 2\omega(1+e)^2 - 12c\cos 2\omega(5e^2+8e+3) \\ -3(8e^2+9e+2)\} + \cos 2\omega\{8c^2\cos^2 2\omega(1+e^2) + 6c\cos 2\omega(3e^2+4e+1) + 3e(1+2e)\} \end{array}\right],$$
$$R_7 = \frac{-c\sin 2\omega}{1536(1+e)^3}\left[\begin{array}{l} 16c^2\sin^3 2\omega\{32c^2\cos 2\omega(27e^3+71e^2+61e+17) + 3(177e^3+391e^2+271e+57)\} \\ -16c\cos 2\omega\{256c^2(1+e)^3\cos^2 2\omega + 48c\cos 2\omega(19e^3+47e^2+37e+9) \\ +3(227e^3+421e^2+221e+27)\} - 3(407e^3+431e^2+61e-3) \end{array}\right],$$
$$R_8 = \frac{c}{24(1+e)^3}\left[\begin{array}{l} c\sin^2 2\omega\{c^2\sin^2 2\omega(113e^3+255e^2+183e+41) - 24c^2\cos^2 2\omega(13e^3+33e^2+27e+7) \\ -6c\cos 2\omega(61e^3+123e^2+75e+13) - 3(30e^3+42e^2+15e+1)\} \\ +\cos 2\omega\{16c^3(1+e)^3\cos^3 2\omega + 24\cos^2 2\omega(3e^3+7e^2+5e+1) \\ +3c\cos 2\omega(25e^3+39e^2+15e+1) + 3e^2(5e+3)\} \end{array}\right].$$

$$V_1 = -\frac{e}{2s^2(1+e)}, \qquad V_2 = \frac{(2e+1)e^2}{8s^4(1+e)^4},$$

$$V_3 = \frac{-(2e^2+e+1)e^3}{16s^6(1+e)^6}, \qquad V_4 = \frac{(3+12e+12e^2+8e^3)e^4}{128s^8(1+e)^8}.$$

$$H_0 = 1+FA, \qquad H_1 = FBkT_1, \qquad H_2 = FAk^2T_2, \qquad H_3 = FBk^3T_3,$$

ISSN(Online) : 2319-8753
ISSN (Print) : 2347-6710

International Journal of Innovative Research in Science, Engineering and Technology

(An ISO 3297: 2007 Certified Organization)

Vol. 5, Issue 4, April 2016

$H_4 = FAk^4T_4$, $H_5 = FBk^5T_5$, $H_6 = FAk^6T_6$, $H_7 = FBk^7T_7$ $H_8 = FAk^8T_8$

$$k = \sqrt{\frac{1-e}{1+e}},$$

$$T_1 = \frac{3e^4 + 4e^3 + 4e^2 + 8e + 8}{8}, \qquad T_2 = -\left[\frac{1 + 2e + 2e^2 + 2e^3 + 2e^4}{2}\right],$$

$$T_3 = -\left[\frac{8 + 40e + 68e^2 + 84e^3 + 99e^4}{64}\right], \qquad T_4 = \frac{7e^4 + 5e^3 + 3e^2 + e}{4},$$

$$T_5 = \frac{1597e^4 + 924e^3 + 380e^2 + 56e - 8}{1024}, \qquad T_6 = -\left[\frac{e^2 + 4e^3 + 9e^4}{8}\right]$$

$$T_3 = -\left[\frac{8 - 24e + 196e^2 + 1716e^3 + 5411e^4}{8192}\right], \qquad T_8 = \frac{5e^4 + e^3}{16}.$$

Appendix-II

$$P_0 = F_0W_0 \qquad P_1 = F_1W_0$$

$$P_2 = F_0W_1 + F_2W_0 \qquad P_4 = F_0W_2 + F_2W_1 + F_4W_0$$

$$P_5 = F_1W_2 + F_3W_1 + F_5W_0 \qquad P_6 = F_0W_3 + F_2W_2 + F_4W_1 + F_4W_0$$

$$P_7 = F_1W_3 + F_3W_2 + F_5W_1 + F_7W_0 \qquad P_8 = F_0W_4 + F_2W_3 + F_4W_2 + F_6W_1$$

$$W_0 = \frac{\sqrt[3]{(1+e)}}{\sqrt{(1-e)}}, \qquad W_1 = \frac{3e^2 - 8e + 1}{8\sqrt{1-e^2}}, \qquad W_2 = \frac{-\left(5e^4 - 16e^3 - 50e^2 + 16e - 3\right)}{128(1+e)^2\sqrt{1-e^2}}$$

$$W_1 = \frac{3e^2 - 8e + 1}{8\sqrt{1-e^2}}, \qquad W_2 = \frac{-\left(5e^4 - 16e^3 - 50e^2 + 16e - 3\right)}{128(1+e)^2\sqrt{1-e^2}},$$

$$W_3 = \frac{\left(7e^6 - 24e^5 - 243e^4 - 80e^3 + 45e^2 - 24e + 5\right)}{1024(1+e)^4\sqrt{1-e^2}},$$

$$W_4 = \frac{-\left(45e^8 - 160e^7 - 4228e^6 - 4128e^5 - 418e^4 + 32e^3 - 228e^2 + 160e - 35\right)}{32768(1+e)^6\sqrt{1-e^2}},$$

ISSN(Online) : 2319-8753
ISSN (Print) : 2347-6710

International Journal of Innovative Research in Science, Engineering and Technology

(An ISO 3297: 2007 Certified Organization)

Vol. 5, Issue 4, April 2016

$$M_0 = F_0 S_0 , \qquad M_1 = F_0 S_1 + F_1 S_0 ,$$

$$M_2 = F_0 S_2 + F_1 S_1 + F_2 S_0 , \qquad M_3 = F_0 S_3 + F_1 S_2 + F_2 S_1 + F_3 S_0 ,$$

$$M_4 = F_0 S_4 + F_1 S_3 + F_2 S_2 + F_3 S_1 + F_4 S_0 ,$$

$$M_5 = F_0 S_5 + F_1 S_4 + F_2 S_3 + F_3 S_2 + F_4 S_1 + F_5 S_0$$

$$M_6 = F_0 S_6 + F_1 S_5 + F_2 S_4 + F_3 S_3 + F_4 S_2 + F_5 S_1 + F_6 S_0$$

$$M_7 = F_0 S_7 + F_1 S_6 + F_2 S_5 + F_3 S_4 + F_4 S_3 + F_5 S_2 + F_6 S_1 + F_7 S_0$$

$$M_8 = F_0 S_8 + F_1 S_7 + F_2 S_6 + F_3 S_5 + F_4 S_4 + F_5 S_3 + F_6 S_2 + F_7 S_1 + F_8 S_0$$

$$S_0 = \left(R_{0i} + R_{2i} + R_{4i}\right) K ,$$

$$S_1 = eR_{1i} + R_{3i} + R_{5i} + R_{6i} ,$$

$$S_2 = -\left[\frac{\left(-15e^2 + 4e + 5\right)R_{0i} + \left(-3e^2 + 4e + 3\right)R_{2i} + \left(e^2 + 4e - 1\right)R_{4i}}{8\left(1+e\right)^2}\right] K ,$$

$$S_3 = \frac{\left(3e^3 - 3e^2 - 3e\right)R_{1i} - 3eR_{3i} + \left(-e^2 - 3e + 1\right)R_{5i} + \left(2e^2 - 3e - 2\right)R_{6i}}{6\left(1+e\right)^2} ,$$

$$S_4 = \left[\frac{\left(35e^4 - 88e^3 - 54e^2 + 120e + 35\right)R_{0i} + \left(-5e^4 + 8e^3 + 26e^2 + 24e - 5\right)R_{2i} + \left(3e^4 + 40e^3 + 10e^2 - 8e + 3\right)R_{4i}}{128\left(1+e\right)^4}\right] K ,$$

$$S_5 = -\left[\frac{\left(-15e^3 - 30e^2\right)R_{1i} + \left(-30e^3 - 15e^2\right)R_{3i} + \left(-4e^4 - 40e^3 - 7e^2 + 10e - 4\right)R_{5i} + \left(6e^4 - 10e^3 - 27e^2 - 20e + 6\right)R_{6i}}{120\left(1+e\right)^4}\right] ,$$

ISSN(Online) : 2319-8753
ISSN (Print) : 2347-6710

International Journal of Innovative Research in Science, Engineering and Technology

(An ISO 3297: 2007 Certified Organization)

Vol. 5, Issue 4, April 2016

$$S_6 = -\left[\frac{\begin{array}{l}(21e^6 - 2125e^5 - 175e^4 + 264e^3 + 303e^2 + 140e - 21)R_{0i} \\ +(-7e^6 + 12e^5 + 101e^4 + 200e^3 + 27e^2 - 20e + 7)R_{2i} \\ +(5e^6 + 172e^5 + 129e^4 + 8e^3 - e^2 + 12e - 5)R_{4i}\end{array}}{1024(1+e)^6}\right]K,$$

$$S_7 = \left[\frac{\begin{array}{l}(-105e^5 - 315e^4 - 105e^3)R_{1i} + (-210e^5 - 210e^4 - 105e^3)R_{3i} \\ +(-12e^6 - 308e^5 - 209e^4 + 21e^3 - e^2 - 28e + 12)R_{5i} \\ +(16e^6 - 28e^5 - 188e^4 - 329e^3 - 22e^2 - 42e - 16)R_{6i}\end{array}}{1680(1+e)^6}\right],$$

$$S_8 = \left[\frac{\begin{array}{l}(99e^8 - 3056e^7 - 3884e^6 + 1424e^5 + 6802e^4 + 7088e^3 + 724e^2 - 336e + 99)R_{0i} \\ +(-45e^8 + 80e^7 + 1556e^6 + 4816e^5 + 2354e^4 + 112e^3 + 20e^2 + 112e - 45)R_{2i} \\ +(35e^8 + 2832e^7 + 3540e^6 + 2192e^5 + 274e^4 + 176e^3 - 44e^2 - 80e + 35)R_{4i}\end{array}}{32768(1+e)^8}\right]K,$$

$$R_{0i} = e\frac{(\mu P_{0i} - aQ_{0i})}{2}, \quad R_{1i} = \mu P_{1i} - aQ_{1i}, \quad R_{2i} = a(Q_{0i} - eQ_{2i}) + \mu(eP_{2i} + p_{0i}),$$

$$R_{3i} = \mu P_{1i} + aQ_{1i}, \quad R_{4i} = a\left(Q_{2i} - e\frac{Q_{0i}}{2}\right) + \mu\left(P_{2i} + e\frac{p_{0i}}{2}\right),$$

$$R_{5i} = \mu P_{3i}, \quad R_{6i} = e\mu P_{3i}.$$